Journal of Steroid Biochemistry and Molecular Biology 194 (2019) 105457

Contents lists available at ScienceDirect

Journal of Steroid Biochemistry and Molecular Biology

journal homepage: www.elsevier.com/locate/jsbmb

Bivalent furostene carbamates as antiproliferative and antiinflammatory agents

Nandini Pathak[a,1], Kaneez Fatima[a,b,1], Sneha Singh[a], Divya Mishra[a], Amit Chand Gupta[a], Yogesh Kumar[a], Debabrata Chanda[a,b], D.U. Bawankule[a,b], Karuna Shanker[a,b], Feroz Khan[a,b], Atul Gupta[a,b], Suaib Luqman[a,b,*], Arvind S. Negi[a,b,*]

[a] CSIR-Central Institute of Medicinal and Aromatic Plants (CSIR-CIMAP), P.O. CIMAP, Kukrail Picnic Spot Road, Lucknow, 226 015, Uttar Pradesh, India
[b] Academy of Scientific and Innovative Research (AcSIR), Ghaziabad, 201002, Uttar Pradesh, India

ARTICLE INFO

Keywords:
Dioscorea floribunda
Anticancer
Apoptosis
Caspase
Ehrlich ascites carcinoma
Acute oral toxicity

ABSTRACT

Breast cancer is the most prevalent cancer in women affecting about 12% of world's female population. It is a multifactorial disease, mostly invasive in nature. Diosgenin and related compounds are potent antiproliferative agents. Carbamate derivatives have been synthesized at C26 of furostene ring after opening spiroketal bond (F-ring) of diosgenin. Compound **10** possessed significant antiproliferative activity against human breast cancer cells by arresting the population at G1 phase of cell division cycle and induced apoptosis. Induction of apoptosis was observed through the caspase signalling cascade by activating caspase-3. Moreover, carbamate **10** exhibited moderate antiinflammatory activity by decreasing the expression of cytokines, TNF-α and IL-6 in LPS-induced inflammation in primary macrophage cells. Furthermore, compound **10** significantly reduced Ehrlich ascites carcinoma significantly in mice. It was well tolerated and safe in acute oral toxicity in Swiss albino mice. The concomitant anticancer and antiinflammatory properties of carbamate **10** are important and thus, can further be optimized for a better anti-breast cancer candidate.

1. Introduction

Breast cancer is one of the most leading causes of deaths in women [1]. Breast cancer possesses heterogeneous population of diverse biomarkers with distinct morphological and phenotypic difference in tumour cells [2]. The heterogeneity in breast tumour cells causes significant challenges in designing effective treatment strategies [3]. Triple negative breast cancer (TNBC) is characterised by the absence of estrogen receptor (ER), progesterone receptor (PgR) and human epidermal growth factor receptor 2 (HER2) [4]. It accounts about 15–20% of all breast cancer cases. Due to poor prognosis and limited response to chemotherapy, TNBC is the most aggressive type of breast cancer [5]. Clinically, there is no well established targeted therapy, only combined 'Omics' approach has been tried to treat the unrevealed TNBC phenotypic heterogeneity. Hence, it is very difficult for clinicians to get proper outcome of the treatment. However, a better understanding about the tumour biomarkers in the heterogeneity would help in designing new chemotherapeutics for TNBC patients. There are mixed treatment options for such type of cancer like antimitotic drugs, taxanes (paclitaxel, docetaxel), DNA cross-linking drugs, platinum complexes (cisplatin, carboplatin), and anthracyclines (doxorubicin), antimetabolites (5-fluorouracil) *etc.* (Fig. 1) [6]. Recently, olaparib, a PARP inhibitor has been approved by US-FDA for certain type of HER2 negative breast cancers [7].

In the present study, the basic furostene core was obtained from diosgenin which is abundantly present in *Dioscorea spp.* Dioscorea is a tuberous herbaceous perennial plant having more than 600 species including *D. alata*, *D. angustifolia*, *D. bulbifera*, *D. glabra*, *D. japonica*, *D. lanata*, *D. villosa*, *D. floribunda etc.* Its tubers are rich in several saponins

Abbreviations: APCI-TOF-MS, Atmospheric Pressure Chemical Ionisation-Time of Flight Mass Spectrometry; $CDCl_3$, Deuterated chloroform; DMAP, Dimethylaminopyridine; ESI-MS, Electrospray Mass Ionisation-Mass Spectrometry; EAC, Ehrlich Ascites Carcinoma; HRMS, High Resolution Mass Spectrometry; HER 2, Human Epidermal growth factor Receptor 2; IL-6, Interleukin 6; IAEC, Institutional Animal Ethical Committee; LPS, Lipopolysaccharide; LC–MS, Liquid Chromatography-Mass Spectrometry; MeOH, Methanol; RT, Room Temperature; SI, Selectivity Index; TNF, Tumour Necrosis Factor; UPLC, Ultra Performance Liquid Chromatography

* Corresponding authors.
E-mail addresses: s.luqman@cimap.res.in (S. Luqman), arvindcimap@rediffmail.com (A.S. Negi).
[1] Equal authorship.

https://doi.org/10.1016/j.jsbmb.2019.105457
Received 2 May 2019; Received in revised form 20 August 2019; Accepted 23 August 2019
Available online 24 August 2019
0960-0760/

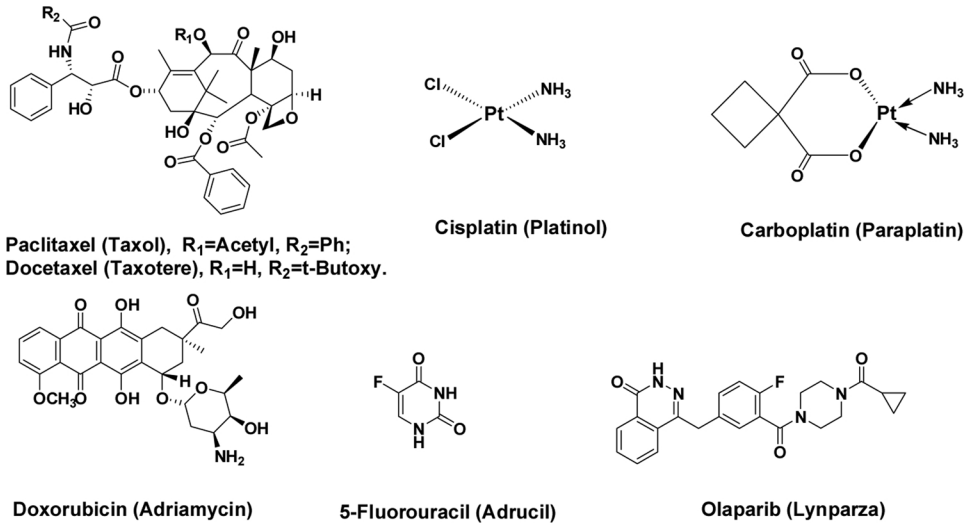

Fig. 1. Some of the clinical drugs in use for the treatment of Triple negative breast cancer.

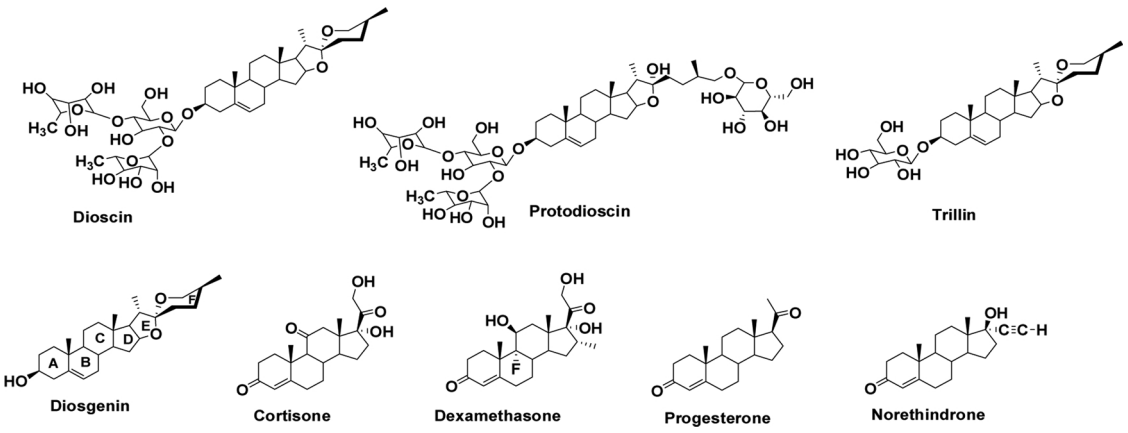

Fig. 2. Saponins from Dioscorea *spp.* and a few important drugs derived from diosgenin.

like dioscin, protodioscin, deltonin, parvifloside, trillin *etc.* Diosgenin is a steroidal aglycon part (sapogenin) of most of these saponins present in good quantity (3–5% approx.). Owing to its high abundance in these plants, diosgenin is used as starting substrate for the synthesis of several high value steroidal clinical drugs like cortisone, progesterone, pregnenolone, dexamethasone [8], prednisolone, metabolic steroids, hormones, vitamins and many contraceptive pills (Fig. 2) [9]. Dioscin exhibited potential antiproliferative activity against various human cancers *i.e.* breast cancer [10], lung cancer [11], hepatocarcinoma [12], gastric cancer [13], leukaemia [14], laryngeal cancer [15] *etc.* Diosgenin (3*β*-hydroxy-5-spirostene), the sapogenin of dioscin has also exhibited several pharmacological activities including anticancer [16], cardioprotective, antidiabetic, anti-inflammatory [17] *etc.* Diosgenin induces apoptosis through modulation of caspase pathway and thus, it interferes cell death pathways [16]. It also inhibits pro-inflammatory cytokines to exhibit anti-inflammatory activity [18]. Specifically, diosgenin exhibited anticancer activity against different types of cancer *i.e.* mammary carcinoma [19], leukaemia [20], hepatocellular [21], colon [22] and cervical cancers [23] *etc.* Further, diosgenin was planned to modify towards furostene framework with carbamate spearhead. Carbamate moiety contributes as a key component towards the improvement of pharmacological and pharmacokinetic properties of drug candidates. In medicinal chemistry, it plays an important role as a drug and prodrug. In our previous studies, we modified diosgenin into anticancer and anti-inflammatory agents [24a,24b,24c]. In the present communication, carbamate derivatives of diosgenin have been evaluated as possible antiproliferative agents.

2. Materials and methods

2.1. General experimentation

Melting points were determined on glass capillaries and are uncorrected. Reagents and other chemicals were purchased from Sigma-Aldrich, USA, Avra Synthesis India, Merck India Ltd. and used without further purification. The reactions were monitored on Merck pre-coated silica gel TLC-GF_{254} aluminium sheets, compounds were visualized under UV light (254 nm and 365 nm) and further charring was done with 2% ceric sulphate in 10% sulphuric acid (aqueous). Pure compounds were characterised by ^{1}H and ^{13}C NMR, ESI-MS, High Resolution Mass on ESI-TOF and APCI-TOF. The NMR spectra were obtained on Bruker Avance III-HD500 MHz instrument with tetramethylsilane (TMS) as an internal standard. Chemical shifts are represented in δ ppm values. ^{1}H–^{1}H coupling constant (J) values are given in Hz. ESI mass spectra were recorded on Shimadzu LC–MS and High Resolution Mass (HRMS) on Agilent 6520Q-TOF after dissolving the compounds in methanol. Dioscin and diosgenin contents were determined by RP-HPLC (Shimadzu, Japan). The purity of final products was checked in Waters UPLC system (Waters, USA). Nomenclature of compounds has been done as per the recommendations by the Joint Commission on Biochemical Nomenclature of IUPAC. [25]

DMEM (Dulbecco's Modified Essential Eagle Medium) and FBS (Fetal Bovine Serum) were procured from Gibco, India. RNase A, Crystal Violet Dye, HEPES, Trypsin-EDTA, MTT dye, Antibiotic-Antimycotic (Ab/Am) Solution, Citric Acid, Propidium Iodide (PI), and

Phosphate Buffer Saline (PBS) were acquired from Merck India Limited (Sigma brand). Sodium bicarbonate ($NaHCO_3$), Sodium Citrate, Di-sodium Hydrogen Phosphate, and Agar were obtained from Himedia Laboratories, India. Solvents including ethanol, DMSO and isopropanol were procured from Merck, India Pvt. Ltd.

2.2. Chemistry

2.2.1. Isolation of dioscin (1) rich fraction and acid hydrolysis to get diosgenin (2)

*Isolation of dioscin (**1**)*: 5.6 Kg of fresh rhizomes of *Dioscorea floribunda* were chopped into small pieces, shade dried and ground to powder (16 No. Sieve). The dried and powdered material (1Kg) was defatted with hexane (3 × 3Lit., 6 h, 6 h, 12 h) and soaked with 90% EtOH-H_2O (4 × 3Lit., 6 h, 12 h, 24 h, 24 h) at room temperature (28–36 °C) to get saponin rich extract (151 g) having dioscin content (4.14% DM, HPLC).

Hydrolysis of saponin: 30 g of saponin rich extract was taken in 90% ethanol-water (50 mL). To this stirred solution 2.5 mL conc. sulphuric acid was added dropwise. The solution was refluxed at 80 °C for 2 h hours. On completion, ethanol was evaporated *in vacuo*. The residue contained 2.92% diosgenin (HPLC). The residue thus obtained was crystallised with chloroform: hexane (2:5) to get 3.62 g pure diosgenin (**2**). It was characterised by m.p. and spectroscopy.

Yield = 1.82% DM; m.p. = 202–204 °C [204–207 °C]; ^{1}H NMR ($CDCl_3$, 500 MHz): δ0.76 (s, 3H, 18-CH_3), 0.95 (d, 6H, 21-CH_3 and 27-CH_3, J = 6.50 Hz), 1.01 (s, 3H, 19-CH_3), 1.06–1.99 (m, 25H, rest of the 1xCH_3, 8xCH_2 and 6xCH of steroidal ring), 2.26 (m, 2H, 7-CH_2), 3.35 (t, 1H, 16-CH, J = 10.5 Hz), 3.46 (m, 2H, 26-CH_2), 4.39 (t, 1H, 3-CH, J = 7.5 Hz), 5.33 (bs, 1H, 6-CH); ^{13}C NMR ($CDCl_3$, 125 MHz): δ14.53 (C21), 16.29 (C18), 17.15 (C27), 19.42 (C19), 20.87 (C11), 28.79 (C2), 30.29 (C25), 31.37 (C23), 31.43 (C15), 31.59 (C24), 31.84 (C8), 32.05 (C7), 36.64 (C10), 37.23 (C1), 39.78 (C4), 40.26 (C13), 41.60 (C20), 42.26 (C12), 50.05 (C9), 56.52 (C14), 62.08 (C17), 66.84 (C26), 71.68 (C3), 80.83 (C16), 109.30 (C22), 121.39 (C6), 140.82 (C5); ESI-MS Mass for $C_{27}H_{42}O_3$ (MeOH): 415 $[M+H]^+$.

2.2.2. Synthesis of (22β,25R)-Spirost-5-en-3β-yl-3β-acetate (3)

Diosgenin (3 g, 7.24 mmol) was taken in dry chloroform (15 mL). To this dimethylaminopyridine (DMAP, 100 mg, 0.82 mmol) and acetic anhydride (2 mL, 2.16 g, 21.16 mmol) were added and the reaction mixture was stirred at room temperature for 4 h. On completion the reaction mixture was extracted with chloroform (30mLx3), acidified with dil. HCl (5%, 10 mL) and washed with water (20 mLx2). The organic layer was dried over anhydrous sodium sulphate and evaporated *in vacuo*.

Yield = 2.21 g (93%); m.p. = 192–194 [195 °C];

^{1}H NMR ($CDCl_3$, 500 MHz): δ0.78 (s, 3H, 18-CH_3), 0.95 (d, 3H, 27-CH_3, J = 7.0 Hz), 1.02 (s, 3H, 19-CH_3), 1.09–1.98 (m, 25H, rest of the 1xCH_3, 8xCH_2 and 6xCH of steroidal ring), 2.02 (s, 3H, CH_3COO, 3-acetate), 2.31 (bs, 2H, 7-CH_2), 3.36 and 3.38 (bs, 2H, 26-CH_2), 4.39 (t, 1H, 16-CH, J = 7.5 Hz), 4.60 (q, 1H, 3-CH), 5.42 (s, 1H, 6-CH); ^{13}C NMR ($CDCl_3$, 125 MHz): δ14.53 (C21), 16.29 (C18), 17.14 (C27), 19.33 (C19), 20.81 (C11), 21.43 (acetate CH_3), 27.74 (C24), 28.81 (C2), 29.71 (C15), 30.30 (C25), 31.41 (C23), 31.84 (C8), 32.04 (C7), 36.74 (C10), 36.96 (C1), 38.09 (C12), 39.73 (C4), 40.26 (C13), 41.62 (C20), 49.94 (C9), 56.43 (C14), 62.08 (C17), 66.85 (C26), 73.90 (C3), 80.81 (C16), 109.29 (C22), 122.37 (C6), 139.69 (C5), 170.55 (Acetate ester); ESI-MS for $C_{29}H_{44}O_4$ (MeOH): 457 $[M+H]^+$.

2.2.3. Synthesis of (22β,25R)-3β,26-dihydroxy furost-5-en-3β-acetate (4)

To a stirred solution of acetyldiosgenin (1 g, 2.19 mmol) in acetic acid: dichloromethane (1:2) (10 mL), sodium cyanoborohydride (600 mg, 9.52 mmol) was added in portions and stirred at room temperature for 2 h. On completion, the reaction was quenched by adding dil. HCl (2%, 20 mL) and extracted with chloroform (20 mLx3). The organic layer was washed with water, dries over anhydrous sodium sulphate and dried *in-vacuo*. The residue thus obtained was purified through column chromatography over silica gel (60–120 mesh) and eluted with hexane-ethyl acetate with increasing polarity of ethyl acetate. The desired alcohol (**4**) was obtained at 20% ethyl acetate-hexane. It was recrystallised with hexane-chloroform (3:1) to get alcohol **4** as crystalline white solid.

Yield = 834 mg (83%); m.p. = 120–122 °C. ^{1}H NMR ($CDCl_3$, 500 MHz): δ0.82 (s, 3H, 18-CH_3), 0.92 (d, 3H, 21-CH_3, J = 6.5 Hz), 0.95 (d, 3H, 27-CH_3, J = 7 Hz),), 0.98 (s, 3H, 19-CH_3), 1.99 (s, 3H, 3-*O*-CO-CH_3, acetate), 1.04–1.88 (m, 22H, rest of the 8xCH_2 and 6xCH of steroidal ring), 2.32 (bs, 2H, 7-CH_2), 3.33 (dt, 1H, 22-CH), 3.44–3.49 (m, 2H, 26-CH_2, J = 6.0 and 6.5 Hz), 4.32 (dt, 1H, 16 − CH, J = 5 Hz), 4.60 (m, 1H, 3-CH), 5.38 (bs, 1H, 6-CH). ^{13}C NMR ($CDCl_3$, 125 MHz): δ16.43, 16.62, 18.91, 19.32, 20.65, 21.41, 27.75, 30.12, 30.45, 31.56, 31.98, 32.22, 35.73, 36.70, 37.00, 37.92, 38.09, 39.41, 40.70, 50.01, 56.90, 65.10, 68.02, 73.89, 83.21, 90.35, 122.37, 139.68, 170.53; ESI Mass for $C_{29}H_{46}O_4$ (MeOH): 459.4 $[M+H]^+$, 481.5 $[M + Na]^+$, 497.5 $[M + K]^+$.

2.2.4. Synthesis of (22β, 25R)-3β-acetoxy, furost-5-en-26-yl-(4-nitrophenyl)-carbonate (5)

To a stirred solution of furostenol derivative **4** (1 g, 2.18 mmol) in dry tetrahydrofuran, sodium hydride (100 mg, 4.17 mmol) (pre-washed with petroleum ether) was added. After stirring for five min., 4-nitrophenylchloroformate (1.2 g, 5.97 mmol) was added in portions. The reaction mixture was stirred for 8 h at room temperature. On completion, water (20 mL) was added to it and extracted with ethyl acetate (20 mLx3), washed with water and dried over anhydrous sodium sulphate. Organic layer was dried *in vacuo*. The residue was recrystallized with chloroform:hexane (1:3) to get pure carbonate derivative **5** as light yellow amorphous solid.

Yield = 1.24 g (91%), m.p. = 109–111 °C; ^{1}H NMR ($CDCl_3$, 500 MHz): δ0.80 (s, 3H, 18-CH_3), 0.99 (d, 3H, 21-CH_3, J = 7 Hz), 1.02 (d, 3H, 27-CH_3, J = 7 Hz), 1.03 (s, 3H, 19-CH_3), 2.04 (s, 3H, 3-*O*-CO-CH_3, acetate), 1.12–2.02 (m, 22H, rest of the 8xCH_2 and 6xCH of steroidal ring), 2.32 (bs, 2H, 7-CH_2), 3.32 (td, 1H, 22-CH), 4.09 and 4.20 (m, 2H, 26-CH_2, J = 5.5 Hz and 6.5 Hz), 4.30 (dt, 1H, 16-CH), 4.60 (bs, 1H, 3-CH), 5.38 (bd, 1H, 6-CH, J = 5 Hz); ^{13}C NMR ($CDCl_3$, 125 MHz): δ 16.45, 16.54, 16.77, 18.90, 19.33, 20.64, 21.43, 27.75, 30.14, 30.65, 31.85, 31.99, 32.23, 37.00, 37.92, 38.09, 39.39, 49.98, 56.89, 65.05, 73.89, 74.24, 83.28, 90.01, 121.80, 122.36, 125.29, 139.71, 145.34, 152.61, 155.64, 170.57; ESI-MS (MeOH): 624.7 $[M+H]^+$, 646.7 $[M + Na]+$, 662.6 $[M + K]^+$.

2.2.5. General procedure for the synthesis of diosgenin derived carbamates synthesis of (22β, 25R)-3β-acetoxy, furost-5-en-26-yl-N,N-dimethyl-carbamate (6)

To a stirred solution of carbonate derivatives **5** (200 mg, 0.32 mmol) in dry dichloromethane (10 mL), triethylamine (1 mL, 7.19 mmol) and dimethylamine (0.8 mL, 11.91 mmol) were added. The reaction mixture was further stirred for 2 h at room temperature. On completion, solvent was evaporated and residue was taken in water (10 mL) and extracted with chloroform (20 mLx3). Organic layer was dried over anhydrous sodium sulphate and evaporated under reduced pressure. The crude mass was purified through column chromatography over silica gel (60–120 mesh) using hexane-ethyl acetate as eluants. The desired carbamate **6** was obtained at 20% ethyl acetate: hexane as light yellow amorphous solid.

Yield = 131 mg (77%), m.p. = 69–71 °C; ^{1}H NMR ($CDCl_3$, 500 Hz): δ 0.77 (s, 3H, 18-CH_3), 0.91(d, 3H, 21-CH_3, J = 6.5 Hz), 0.95 (d, 3H, 27-CH_3, J = 6.5 Hz), 1.00 (s, 3H, 19-CH_3), 1.99 (s, 3H, 3-*O*-CO-CH_3, acetate), 1.04–1.96 (m, 22H, rest of the 8xCH_2 and 6xCH of steroidal ring), 2.29 (bs, 2H, 7-CH_2), 2.87 (s, 6H, N-$(CH_3)_2$), 3.30 (bs, 1H, 22-CH), 3.84 and 3.92 (m, 2H, 26-CH_2, J = 5.5 Hz and 6.5 Hz), 4.27 (bs, 1H, 16-CH), 4.52 (bs, 1H, 3-CH), 5.33 (bs, 1H, 6-CH); ^{13}C NMR ($CDCl_3$, 125 MHz): δ16.39, 16.85, 18.92, 19.30, 20.63, 21.36, 27.73, 29.66, 30.45, 30.84, 31.56, 31.97, 32.21, 33.13, 36.69, 36.99, 37.91, 38.08, 39.39, 40.66, 50.01, 56.89, 65.15, 70.20, 73.87, 77.28, 83.16, 90.21,

122.34, 139.67, 156.86, 170.47; ESI Mass for $C_{32}H_{51}NO_5$, (MeOH): 552 $[M + Na]^+$.

2.2.6. (22β,25R)-3β-acetoxy, furost-5-en-26-yl-N-(n)-propylcarbamate (7)

Yield = 73%, m.p. = oil ^{1}H NMR ($CDCl_3$, 500 Hz): δ 0.79 (s, 3H, 18-CH_3), 0.92(d, 3H, 21-CH_3, J = 6.5 Hz), 0.97 (d, 3H, 27-CH_3, J = 6.5 Hz),), 1.03 (s, 3H, 19-CH_3), 2.01 (s, 3H, 3-*O*-CO-CH_3, acetate), 1.12 (t, 3H, CH_3, J = 10 Hz), 1.14–1.95 (m, 24H, rest of the 8xCH_2 and 6xCH of steroidal ring and 2'-CH_2 of carbamate chain), 2.32 (bs, 2H, 7-CH_2), 3.13 (bt, 2H, N-CH_2, J = 6.5 Hz), 3.30 (dt, 1H, 22-CH, J = 8 Hz and 4 Hz), 3.84 and 3.94 (m, 2H, 26-CH_2, J = 7 Hz and 5.5 Hz), 4.29 (q, 1H, 16-CH, J = 5.5 Hz and 5 Hz), 4.59 (m, 1H, 3-CH, J = 5.5 Hz and 5 Hz), 5.36 (bd, 1H, 6-CH, 5 Hz); ^{13}C NMR ($CDCl_3$, 125 MHz): δ 12.00, 17.02, 18.94, 19.33, 50.65, 21.42, 27.75, 29.36, 29.70, 30.43, 30.51, 30.84, 31.58, 31.92, 31.99, 32.23, 33.16, 36.72, 37.00, 37.91, 38.09, 39.41, 40.69, 42.69, 50.01, 56.90, 65.14, 73.91, 83.20, 90.24, 122.38, 139.70, 156.90, 170.56; APCI-TOF-HRMS for $C_{33}H_{53}NO_5$ (MeOH): calc: 544.4001 $[M+H]^+$, obsd: 544.3995.

2.2.7. (22β,25R)-3β-acetoxy, furost-5-en-26-yl-pyrrolidin-1-carboxylate (8)

Yield = 72%, m.p. = 84–86 °C; ^{1}H NMR ($CDCl_3$, 500 Hz): δ 0.79 (s, 3H, 18-CH_3), 0.92 (d, 3H, 21-CH_3, J = 6.5 Hz), 0.97 (d, 3H, 27-CH_3, J = 6.5 Hz),), 1.02 (s, 3H, 19-CH_3), 1.12 (t, 4H, 2xCH_2 of pyrrolidine ring), 2.02 (s, 3H, 3-*O*-CO-CH_3, acetate), 1.09-1.99 (m, 22H, rest of the 8xCH_2 and 6xCH of steroidal ring), 2.31 (bs, 2H, 7-CH_2), 3.26 (t, 4H, N-$(CH_2)_2$, J = 5.5 Hz), 3.86 and 3.96 (m, 2H, 26-CH_2), 4.10 (bs, 1H, 22-CH), 4.20 (bs, 1H, 16-CH), 4.52 (bs, 1H, 3-CH), 5.36 (bs, 1H, 6-CH).; ^{13}C NMR ($CDCl_3$, 125 MHz): δ14.19, 16.42, 16.88, 18.94, 18.95, 19.32, 20.65, 21.40, 27.75, 30.50, 30.90, 31.58, 31.99, 31.99, 32.23, 33.21, 36.71, 37.00, 37.94, 38.09, 39.41, 40.68, 45.66, 46.07, 50.02, 56.90, 60.37, 65.16, 69.76, 73.89, 83.17, 90.27, 122.36, 139.70, 155.35, 170.51; ESI Mass for $C_{34}H_{53}NO_5$ (MeOH): 556 $[M+H]^+$, 594 $[M + K]^+$; APCI-TOF-HRMS Mass for $C_{34}H_{53}NO_5$ (MeOH): cacl: 556.4001 $[M+H]^+$, obsd: 556.3995.

2.2.8. (22β,25R)-3β-acetoxy, furost-5-en-26-yl-piperidin-1-carboxylate (9)

Yield = 61%, m.p. = 121–123 °C; ^{1}H NMR ($CDCl_3$, 500 Hz): δ 0.78 (s, 3H, 18-CH_3), 0.92 (d, 3H, 21-CH_3, J = 6.5 Hz), 0.98 (d, 3H, 27-CH_3, J = 6.5 Hz), 1.02 (s, 3H, 19-CH_3), 1.13 (m, 6H, 3xCH_2 of piperidine ring), 2.01 (s, 3H, 3-*O*-CO-CH_3, acetate), 1.08–1.98 (m, 22H, rest of the 8xCH_2 and 6xCH of steroidal ring), 2.31 (m, 2H, 7-CH_2, J = 5 Hz), 3.39 (t, 4H, N-$(CH_2)_2$, J = 5.3 Hz), 3.85 and 3.94 (d, 2H, 26-CH_2, J = 7 Hz and 5.5 Hz), 4.30 (bs, 1H, 22-CH), 4.64 (bs, 1H, 16-CH), 4.52 (bs, 1H, 3-CH), 5.35 (bs, 1H, 6-CH); ^{13}C NMR ($CDCl_3$, 125 MHz): δ 11.22, 14.12, 16.43, 18.95, 20.65, 22.70, 24.45, 27.29, 29.85, 30.55, 30.90, 31.57, 31.87, 31.93, 32.23, 36.69, 37.00, 37.94, 39.40, 46.04, 50.00, 56.89, 65.13, 70.01, 73.88, 83.18, 90.25, 114.08, 122.39, 139.26, 139.68, 155.69, 170.53; APCI-TOF-HRMS for $C_{35}H_{55}NO_5$ (MeOH): calc: 570.4158 $[M+H]^+$, obs.: 570.4155.

2.2.9. (22β,25R)-3β-acetoxy, furost-5-en-26-yl-(N-methylpiperazin)-1-carboxylate (10)

Yield = 66%, m.p. = 73–75 °C; ^{1}H NMR ($CDCl_3$, 500 Hz): δ 0.78 (s, 3H, 18-CH_3), 0.92(d, 3H, 21-CH_3, J = 6.5 Hz), 0.98 (d, 3H, 27-CH_3, J = 6.5 Hz), 1.02 (s, 3H, 19-CH_3), 2.01 (s, 3H, 3-*O*-CO-CH_3, acetate), 1.09–1.99 (m, 22H, rest of the 8xCH_2 and 6xCH of steroidal ring), 2.28 (s, 3H, N-CH_3), 2.35 (bs, 2H, 7-CH_2), 3.30 (bs, 1H, 22-CH), 3.48 (bs, 8H, N-$(CH_2)_4$), 3.84 and 3.95 (d, 2H, 26-CH_2, J = 7 Hz and 5.5 Hz), 4.28 (bs, 1H, 16-CH), 4.60 (bs, 1H, 3-CH), 5.36 (bd, 1H, 6-CH, J = 5 Hz).; ^{13}C NMR ($CDCl_3$, 125 MHz): δ 16.44, 16.88, 18.95, 19.33, 20.64, 21.42, 27.74, 29.69, 30.49, 30.84, 31.57, 31.92, 31.99, 32.23, 36.71, 36.99, 37.92, 39.40, 40.68, 46.16, 50.00, 54.73, 56.89, 65.12, 70.26, 73.88, 83.20, 90.20, 122.37, 139.26, 139.69, 155.56, 170.53; ESI Mass for $C_{35}H_{56}N_2O_5$ (MeOH): 585 $[M+H]^+$, 543 $[(M\text{-}CH_2CO)+H]^+$; ESI-HRMS for $C_{35}H_{56}N_2O_5$, $[M+H]^+$ calc: 585.4289; obs.: 585.4258.

2.2.10. (22β,25R)-3β-acetoxy, furost-5-en-26-yl-morpholin-1-carboxylate (11)

Yield = 73%, m.p. = 140-142 °C; ^{1}H NMR ($CDCl_3$, 500 Hz): δ 0.78 (s, 3H, 18-CH_3), 0.92 (d, 3H, 21-CH_3, J = 6.5 Hz), 0.98 (d, 3H, 27-CH_3, J = 6.5 Hz), 1.02 (s, 3H, 19-CH_3), 2.01 (s, 3H, 3-*O*-CO-CH_3, acetate), 1.04-1.97 (m, 22H, rest of the 8xCH_2 and 6xCH of steroidal ring), 2.31 (bs, 2H, 7-CH_2), 3.28 (bs, 1H, 22-CH), 3.45 (s, 4H, *N*-$(CH_2)_2$), 3.63 (bs, 4H, *O*-$(CH_2)_2$), 3.87 and 3.97 (d, 2H, 26-CH_2, J = 10 Hz and 7 Hz), 4.28 (bs, 1H, 16-CH), 4.58 (bs, 1H, 3-CH), 5.35 (bs, 1H, 6-CH); ^{13}C NMR ($CDCl_3$, 125 MHz): δ 16.38, 16.79, 18.87, 19.28, 20.60, 21.36, 27.70, 29.64, 30.41, 30.75, 31.53, 31.94, 32.18, 33.01, 36.66, 36.95, 37.89, 38.05, 39.36, 40.64, 49.96, 56.85, 65.07, 66.58, 70.35, 73.84, 83.16, 90.11, 122.32, 139.65, 155.58, 170.47; ESI Mass for $C_{34}H_{53}NO_6$ (MeOH): 594 $[M + Na]^+$.

2.2.11. (22β,25R)-3β-acetoxy, furost-5-en-26-yl-[4-N(2-methoxyphenyl)-piperazin]-1-carboxylate (12)

Yield = 52%, m.p. = oil; ^{1}H NMR ($CDCl_3$, 500 Hz): δ 0.79 (s, 3H, 18-CH_3), 0.94 (d, 3H, 21-CH_3, J = 7 Hz), 0.99 (d, 3H, 27-CH_3, J = 6.5 Hz), 1.02 (s, 3H, 19-CH_3), 2.02 (s, 3H, 3-*O*-CO-CH_3, acetate), 1.09-1.99 (m, 22H, rest of the 8xCH_2 and 6xCH of steroidal ring), 2.31 (bs, 2H, 7-CH_2), 3.00 (s, 4H, *N*-$(CH_2)_2$), 3.30 (bs, 1H, 22-CH), 3.64 (bs, 4H, O-CO-N-$(CH_2)_2$), 3.86 (s, 3H, OCH_3), 3.89 and 3.98 (bs, 2H, 26-CH_2), 4.26 (bs, 1H, 16-CH), 4.59 (bs, 1H, 3-CH), 5.38 (bs, 1H, 6-CH), 6.86-6.99 (m, 4H, 4xCH aromatic); ^{13}C NMR ($CDCl_3$, 125 MHz): δ16.42, 16.82, 18.96, 19.33, 20.65, 21.42, 26.48, 27.75, 29.69, 30.48, 30.81, 31.58, 31.99, 36.71, 37.00, 37.92, 38.10, 39.40, 40.69, 50.62, 50.66, 55.41, 56.89, 64.63, 65.13, 70.28, 73.90, 83.20, 90.19, 111.33, 118.42, 121.03, 122.29, 122.38, 123.39, 123.44, 139.68, 141.03, 152.28, 155.64, 170.53; ESI Mass for $C_{41}H_{60}N_2O_6$ (MeOH): 699 $[M + Na]^+$.

*2.2.12. Purity profile of compound **10** by UPLC*

A simple gradient reverse phase ultra-performance liquid chromatographic (RP-UPLC) method was developed for the determination of purity of compound **10** in the presence of its possible process impurities and storage degradation products. Liquid chromatographic system was an ACQUITY-UPLC H-Class Biosystem (Waters, USA) equipped with a PDA detector (set at 205 nm). The UPLC column was C-18 (BEH 130 Å, 1.7 × 50 mm, 1.7 μm (Waters, Milford, USA). The binary mobile phases were A (water with 0.1% formic acid) and B (acetonitrile). The UPLC thermostat (35 ± 0.1 °C) column was eluted with a gradient from 10% to 90% B in 5 min, and held for 10 min at a flow rate of 0.3 mL/min. The injection volume was 3.0 μL. The purity of the compounds was calculated by UPLC peak area normalization method due non-availability of reference with defined potency.

2.3. Biological evaluation

2.3.1. Cell culture

The human cancer cell lines *i.e.* MCF-7 (Breast cancer, hormone dependent), MDA-MB-231 (Breast cancer, triple negative), PC-3 (Prostate cancer), Colo-205 (Colon cancer), Jurkat (Leukaemia), A549 (Lung cancer), HepG-2 (Liver cancer) and HEK-293 (Human Embryonic Kidney) were originally obtained from National Centre for Cell Science, Pune, India and grown at 37 °C in DMEM supplemented with 10% FBS and Ab/Am (antibiotic-antimitotic) solution in a CO_2 incubator (Thermo Scientific) under 5% CO_2 and 95% relative humidity.

2.3.2. Cell viability assay

The MTT assay was performed as per our previously reported method using above mentioned human cancer cell lines [26]. In brief, 2×10^3 cells/well were incubated in the 5% CO_2 incubator for 24 h to enable them to adhere properly to the 96 well polystyrene microplates (Grenier, Germany). The carbamate derivatives (**6**-**12**) and standard drugs (doxorubicin and cisplatin) were dissolved in dimethylsulphoxide (DMSO, Merck, India), in at least three concentrations and added into

the wells and incubated for 24 h in the CO_2 incubator at 37 °C. The concentration of DMSO was always kept below 0.5%, which was found to be non-toxic to the cells. Then, 10 μL of MTT [3-(4,5-dimethylthiazol-2-yl)-2,5-diphenyltetrazolium bromide, 5 mg/mL] was added to each well and plates were incubated at 37 °C for 4 h. The formazan crystals were dissolved in 100 μL DMSO to each well by thoroughly mixing. The plates were read on Multiscan GO Microplate reader (Thermo Scientific) at 570 nm within 1 h of DMSO addition.

The antiproliferative effect of the compound was calculated as percent inhibition in cell growth as per the formula: [(Absorbance of control-Absorbance of test sample)/(Absorbance of control)] X100

The dose dependent curves were used to determine 50% inhibitory concentration (IC_{50}).

2.3.3. Soft agar colony assay

In this assay, cancer cells were dispersed onto a culture plate (area of 60 mm plate = 2826mm^2) and grown in presence of 'feeder' cells or conditioned medium to provide necessary growth factors. Human breast cancer cell MDA-MB-231 (5×10^4 per mL) were seeded separately in 24 well plates with or without compound **10** treatment for 24 h [27]. A bottom jelly layer was made with 0.72% agar and 4 mL media in a 90 mm Petri dish followed by the formation of top layer with the cells and 3 mL media in 0.36% agar. The petri dishes were incubated in a CO_2 incubator for 15–20 days till the appearance of the colonies followed by staining with Crystal Violet (0.04% in 2% ethanol) and incubation for 1 h at room temperature. After the incubation period, the colony was counted using inverted microscope and pictures were captured accordingly. The experiments were performed in duplicate and results are expressed as Mean ± SD.

2.3.4. Cell cycle analysis

The effect of compound **10** on cell division cycle of MDA-MB-231 cells was assessed by flow cytometry with PI-stained cellular DNA [28]. Briefly, 2×10^6 cells/ mL were grown in a 6 well plate with or without treatment of compound **10** and incubated at 37 °C in 5% CO_2 for 24 h. The cells were collected and washed with PBS followed by fixing in 70% ethanol which was added drop wise through vortexing and kept for overnight at 4 °C. The fixed cells were centrifuged at high rpm to remove ethanol followed by washing with PBS and addition of DNA extraction buffer. The samples were incubated for 5 min at room temperature and centrifuged again to get a pellet which was dissolved in PI staining solution followed by RNaseA (200 μg/mL) treatment and incubated for 30 min at RT. Finally, the cell cycle analysis was done using Flow Cytometer (BD Biosciences LSR II, San Jose, CA, USA) and the analysis was performed through Facs Diva Software, version 6.1.3. The experiments were performed in duplicates and results are expressed as Mean ± SD.

2.3.5. Apoptosis vs necrosis induction by compound *10* by Annexin V-FITC assay

Annexin V-FITC apoptosis assay was done on Flow Cytometer as per the reported method [29]. MDA-MB-231 cells (1×10^6 cells/mL) were seeded in 6-well plate and left overnight before treatment with compound **10** at various concentrations (Half IC_{50}, $IC_{50,}$ and double IC_{50}) for 24 h. All the cells apoptotic and adherent were collected and centrifuged at 5000 rpm for 5 min at 4 °C and washed twice with cold PBS. The pellets were dissolved in 100 μL 1Xbinding buffer and incubated for 15 min with 5 μL of FITC-Annexin V and 5 μL propidium iodide (PI) (as per BD Bioscience Kit Protocol). The samples were maintained with 500 μL 1X binding buffer and stained cells were analysed by FACS Diva software of flow cytometer within 1 h.

Annexin V-FITC binds to phosphatidiylserine present on membrane surface in case of apoptotic cells whereas propidium iodide labelled the cellular DNA in necrotic cell. This combination allows the differentiation among viable cells (Annexin V negative, PI negative), early apoptotic cells (Annexin V positive, PI negative), late apoptotic cells (Annexin V positive, PI positive), and necrotic cells (Annexin V negative, PI positive).

2.3.6. Computational studies

Molecular docking studies were performed to know the binding conformation of ligands in protein active site by docking software AutoDock Vina [30a]. The protein 3D crystallographic structures of Caspase 3 PDB ID: **3KJF** [30b] and Caspase 9 PDB ID: **INW9** [30c] were downloaded from the RCSB PDB database in the PDB format. Protein PDB structures and compound **10** was designed and energy minimized by ChemDraw Ultra 7 molecular editor and Chem3D Pro 7 (Cambridge Soft, PerkinElmer Informatics). The standard drug doxorubicin was used as the positive control. The docking was done by AutoDock Vina, where protein and ligands were kept flexible; the top 10 generated docking poses of all docked compounds were visualized using LigPlot + [30d]. Further, compound **10** was evaluated also for *'Lipinski's rule of five'* to determine the bioavailability of it as orally active drug in humans.

2.3.7. Apoptosis induction by caspase pathway

The **CASP3 (**a **c**ysteine-**asp**artic acid protease) plays a central role in the execution-phase of cell apoptosis [31]. The assay was performed as per the protocol described in caspase-3 human ELISA kit from MyBioSource (Catalog # MBS260710). Doxorubicin and compound **10** (100 μL each) were pipetted into the 96- well plate which was pre-coated with caspase-3 monoclonal antibody, supplied with the kit (cell lysate was prepared after giving 24 h treatment of compound **10** to MDA-MB-231 cells). The plate was sealed with the sealer and incubated at 37 °C for 90 min, thereafter the plate was washed twice with the washing buffer (300 μL) followed by the addition of biotinylated antibody (100 μL) specific to caspase-3. The plate was incubated once again for 1 h and unbound biotinylated antibody was removed by the washing buffer. Further, 100 μL of enzyme-conjugate solution was added and plate was incubated for 30 min at 37 °C. After washing, 100 μL of colour reagent was poured in each well followed by the addition of colour reagent C within 30 min. The colour developed in proportion to the amount of bound caspases-3, the intensity of which was measured at 450 nm immediately [**31**]. All the samples were assayed in duplicate. Doxorubicin was used as a standard inhibitor of caspase. The concentration of caspase-3 in the samples was determined by plotting the absorbance (optical density) of the samples to the equation derived from the standard curve of caspases-3. In addition, we also determined the percent activation and analysed the data by comparing it with the control value.

2.3.8. Anti-inflammatory activity of carbamate *10* against LPS-induced inflammation in primary macrophage cells

The primary macrophage cells were isolated from the peritoneal cavities of mice (8-week-old Swiss albino mice) after an intra-peritoneal injection of 1.0 mL of 1% peptone (BD Biosciences, USA) 3 days before harvesting [24b]. Mice were euthanized after overdose of anaesthesia and peritoneal macrophages were obtained by intra-peritoneal injection of PBS (pH, 7.4). The membrane debris was removed by filtering the cell suspensions through sterile gauze. The viability of cells was determined by trypan blue exclusion and the viable macrophage cells were used at the concentration of 0.5×10^6 live cells/well for the experimentation. The cells were grown in 48 well culture plates in DMEM (Dulbecco modified Eagle medium, Sigma) supplemented with 10% fetal bovine serum with 1Xstabilized antibiotic-antimycotic solution in an incubator at 37 °C in a humidified atmosphere with 5% CO_2. The cells were pre-treated with test compounds (**6** and **10** and doxorubicin at 1 μg/mL and 10 μg/mL) and standard drug (dexamethasone; 1 μg/mL and 10 μg/mL) 30 min before LPS (0.5 μg/mL) stimulation.

TNF-α and IL-6 release in the cell culture supernatant were carried out with EIA Kit following the manufacturer's protocol. Mouse-specific TNF-α and IL-6 Enzyme Immune Assay (EIA) Kits were procured from BD Biosciences, USA. Briefly, the ELISA plates (96 well) were coated (100 μL/well) with mouse-specific TNF-α and IL-6 capture antibody, respectively, and incubated overnight at 4 °C. The plate was blocked with 200 μL/well assay diluents. The culture supernatant and standard (100 μL) were added into the appropriate coated wells and incubated

for 2 h at room temperature (22 ± 3 °C). After incubation, the plates were washed thoroughly 5 times with wash buffer. 100 µL of detecting solution (detection antibody and Streptavidin HRP) was added in to each well. The plate was sealed and then incubated for 1 h at room temperature, and then the plates were washed thoroughly 5 times with a wash buffer. 100 µL of tetramethylbenzidine (TMB) substrate solution was added to each well, and the plate (without plate sealer) was incubated for 30 min at room temperature in the dark. 50 µL of stop solution (2 N H_2SO_4) was then added to each well. The colour density was measured at 450 nm and 570 nm using a microplate reader (Molecular Devices, USA). The absorbance at 570 nm was subtracted from the absorbance at 450 nm. The values of TNF-α and IL-6 were expressed as pg/mL. The percent inhibition of pro-inflammatory cytokine production was calculated as follows:

$$\text{Percent inhibition} = \frac{100\text{x(concentration of vehicle control-concentration of test treatment)}}{\text{OD of concentration of vehicle control}}$$

Where, vehicle control indicates cells treated with vehicle in LPS induced inflammation.

2.3.9. In-vivo efficacy by Ehrlich ascites carcinoma

In vivo anticancer activity of compound **10** was evaluated against Ehrlich Ascites Carcinoma (EAC) model as per the reported method [26]. EAC cells are originally derived from murine mammary tissue and performed by serial intraperitoneal passage in outbred mice. They are undifferentiated and hyper-diploid in nature. Non-inbred Swiss albino mice from our institutional animal house were used for the experiments.

The animals were housed under standard husbandry conditions as per the care and use of laboratory animals. The animals were provided with pelleted feed (M/s Ashirwad Industries, Chandigarh, India) and autoclaved water *ad libitum*. The study and number of animals used were approved by the Institutional Animal Ethics Committee (IAEC) of CSIR-Central Institute of Medicinal and Aromatic Plants, Lucknow, India *via* CIMAP/IAEC/2016-19/32 dated 09-02-2017.

The cells were collected from the peritoneal cavity of Swiss mice harbouring 8–10 days old ascites carcinoma. On day 0, EAC cells (1×10^7) were injected intraperitoneally in non-inbred female Swiss albino mice selected for the experiment. Next day, the animals were randomized and divided into four groups, one vehicle control group, Group-I and three treatment groups, Group-II/Group-III-compound **10** and Group-IV (Standard drug, 5FU)-5 fluorouracil. The first group *i.e.* vehicle control group was administered normal saline (0.2 mL, *i.p.*) for 9 days. The second and third groups were given test compound **10** at 50 and 75 mg/kg *i.p.* doses and the fourth group was given standard drug, 5-fluorouracil at a dose of 20 mg/kg, *i.p.* from day 1–9 and it served as a positive control. On day 12, the animals were sacrificed and ascitic fluid was collected from the peritoneal cavity of each mouse for the evaluation of tumour growth. The percent tumour growth inhibition (TGI) was calculated using the formula described below;

$$\%\text{TGI} = \frac{\text{(Average number of tumour cells in control group} - \text{Average number of tumour cells in test group)}}{\text{Average number of tumour cells in control group}} \times 100$$

2.3.10. Safety studies of carbamate *10* by acute oral toxicity

The study and number of animals used were approved by the Institutional Animal Ethics Committee (IAEC) of CSIR-Central Institute of Medicinal and Aromatic Plants, Lucknow, India *via* CIMAP/IAEC/2016-19/1 dated 09-02-2017.

30 Mice (15 male and 15 female) were taken and divided into four groups comprising 3 male and 3 female mice in each group weighing between 20–25 g. The animals were maintained at 22 ± 5°C with humidity control and also on an automatic dark and light cycle of 12 h. The animals were fed with the standard mice feed and provided *ad libitum* drinking water. Mice of group 1 (Group I) were kept as vehicle control and animals of groups 2, 3, 4 and 5 (Groups II, III, IV & V) were kept as experimentals. The animals were acclimatized for 7 days in the experimental environment prior to the actual experimentation. The test compound **10** was solubilized in dimethylsulphoxide and then suspended in groundnut oil and was given at 5, 50, 300 and 1000 mg/kg body weight to animals of groups 2, 3, 4 and 5 (Groups II, III, IV & V) respectively once orally.

The animals were checked for mortality and any signs of ill health at hourly interval on the day of administration of drug and there after a daily general case side clinical examination was carried out including changes in skin, mucous membrane, eyes, occurrence of secretion and excretion and also responses like lachrymation, pilo-erection respiratory patterns *etc.* Also changes in gait, posture and response to handling were also recorded [32]. In addition to observational study, body weights were recorded and blood and serum samples were collected from all the animals on 7th day of the experiment in acute oral toxicity. The samples were analysed for total RBC, WBC, differential leucocytes count, haemoglobin percentage and biochemical parameters like ALP, SGPT, SGOT, total cholesterol, triglycerides, creatinine, bilirubin, serum protein level. The animals were then sacrificed and were necropsed for any gross pathological changes. The weights of the vital organs like liver, heart, kidney *etc.* were recorded [33].

2.3.11. Statistical analysis

The statistical analysis for the cytotoxicity experiments were carried out using MS-Excel. The anti-inflammatory results were presented as the Mean ± SE and analyzed using GraphPad Prism 5. The ANOVA followed by Tukey's multiple comparison test was used to assess the statistical significance of vehicle *versus* treatment groups. All comparisons are made relative to the untreated controls and significance of differences is indicated as *p value < 0.05 and **p < 0.01.

3. Results

3.1. Chemical synthesis

The schematic diagram of the chemical synthesis is depicted in the Scheme 1. Diosgenin (**2**) was the starting compound which was obtained on acid hydrolysis (5% HCl in MeON-H_2O = 9:1) of dioscin rich extract of rhizomes of *Dioscorea floribunda* in 1.82% yield. 3-Hydroxyl group of **2** was protected as acetyl group using DMAP-acetic anhydride system in dry chloroform at RT to afford 3-acetyldiosgenin (**3**) in 93% yield. The spiroketal bond of **3** was reduced with sodium cyanoborohydride in dichloromethane-acetic acid system (2:1) to open F-ring of diosgenyl acetate to get a primary alcohol (Furostenol derivative) at C26 (**4**) in 78% yield. The alcohol **4** was condensed with 4-nitrophenylchloroformate in the presence of sodium hydride in dry THF to yield a corresponding carbonate derivative **5**. Finally, furostene carbonate derivative (**5**) was treated with various primary or secondary amines in the presence of triethylamine in dry dichloromethane to obtain desired carbamate derivatives (**6-12**) in 52–77% yields. The products were purified through column chromatography and confirmed by spectroscopy [Supplementary information]

3.1.1. Purity profile of compound *10*

Chromatographic conditions were optimised to get optimum separation. The peaks integration performed at λ_{max} (205 nm) due to compound non-chromophoric nature. However, the column eluent monitored in PDA range (190–400 nm) for possible impurities of chromophoric and non-chromophoric both. The peak area and the retention time of compound **10** and other unknown peaks were selection criteria for optimization. Under optimised chromatographic condition, compound **10** eluted at 4.755 min (t_R) while other impurities at 2.544, and 5.743 min without any interference. As a reference method, the functions for peak purity analysis in the chromatographic data processing by chromatography data software (Empower®, Waters, USA) were applied. The purity of compound **10** was 94.79%.

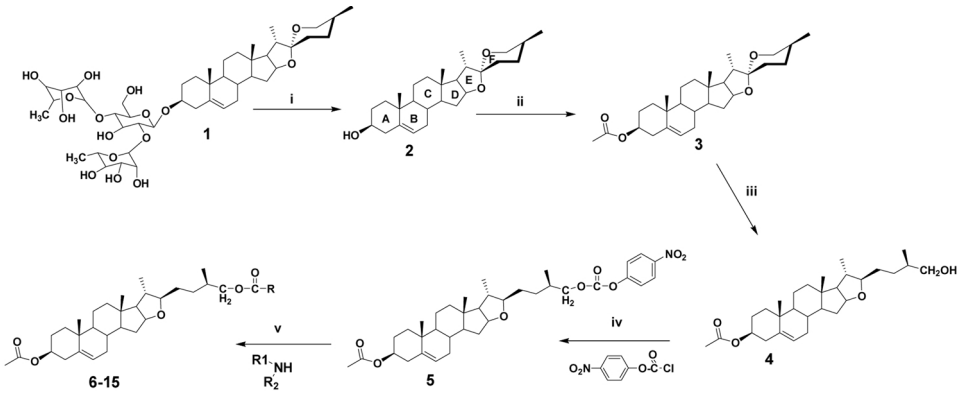

6: R=Me_2N-;
7: R=n-Propyl-NH-;
8: R=Pyrrolidino;
9: R=Piperidino;
10: R=N-methylpiperazino;
11: R=Morpholino;
12: R=N-(2-anisidyl)-piperazino;

Scheme 1. Reagents and conditions: i) 5%H_2SO_4 in 90% ethanol, reflux, 1 h, 82.4%; ii) Ac_2O, DMAP, dry $CHCl_3$, RT, 2 h, 93%; iii) AcOH:DCM = 1:2, $NaCNBH_3$, RT, 1 h, 78%; iv) NaH, dry THF, 4-nitrophenylchloroformate, RT, 8 h, 82%; v) sec-amine, TEA, dry DCM, RT.2–3 h,52–89%.

Table 1
Cytotoxicity of diosgenin based carbamate derivatives against human cancer cell lines.

Compound	Cytotoxicity (IC_{50} in μM)*								Selectivity index IC_{50} (HEK)/IC_{50} (MDA-MB-231)
	MCF-7	MDA-MB-231	PC-3	Colo203	Jurkat	A549	HepG-2	HEK-293	
6	35.61	23.98	> 60	> 60	38.92	> 60	> 60	> 120	5.00 >
7	> 60	> 60	> 60	> 60	> 60	> 60	> 60	> 120	—
8	22.30	> 60	> 60	> 60	> 60	> 60	> 60	> 120	—
9	38.08	> 60	> 60	> 60	> 60	> 60	56.15	> 120	—
10	24.77	**13.52**	> 60	> 60	**15.85**	55.41	32.17	> 120	**8.88** >
11	> 60	> 60	> 60	> 60	> 60	> 60	27.46	> 120	—
12	> 60	> 60	> 60	> 60	> 60	> 60	> 60	> 120	—
Cisplatin	51.06	51.34	67.00	29.00	39.23	38.47	33.74	75.27	1.47
Doxorubicin	01.29	**13.39**	22.52	14.30	—	16.68	—	31.79	2.37

*At 24 h; IC_{50} > 60 μM considered as inactive;

Table 2
Compound **10** effectively inhibits colony formation of MDA-MB-231 cells (no. of seeded cells = 5×10^4 cells/mL, area of 60 mm plate = 2826mm^2).

Compound	Concentration (μg/mL)	Average Live Cells (%)#	MDA-MB-231 (% dead cells)	MDA-MB-231 IC_{50} (μg/mL)
Control	—	100	0	—
10	2	94.08	5.92 ± 2.50	16.33
	10	56.95	43.05 ± 3.27	
	50	38.87	61.13 ± 3.24	
Doxorubicin	0.4	84.73	15.27 ± 4.07	1.28
	2.0	39.35	60.65 ± 5.47	
	10	19.80	80.20 ± 0.06	

* Number of colonies = 2058 ± 74; # n = 2.

3.2. Biological evaluation

3.2.1. Cytotoxicity evaluation

All the diosgenin derived carbamates (compounds **6-12**) were evaluated for antiproliferative activity against a panel of seven human cancer cell lines *i.e.* MCF-7, MDA-MB-231, PC-3, Colo-205, Jurkat, A549, HepG-2 and HEK-293 by employing MTT assay. Out of the ten carbamate derivatives only eight of the derivatives exhibited cytotoxicity (IC_{50} < 60 μM). Compound **10** exhibited moderate cytotoxicity (IC_{50} = 13.52 μM) against MDA-MB-231 and Jurkat cells (IC_{50} = 15.85 μM). The cytotoxicity of compound **10** against triple negative breast cancer cell line *i.e.* MDA-MB-231 was comparable to the standard drug doxorubicin (IC_{50} = 13.39 μM) and a much higher selectivity index (more than 8.88) as compared to cisplatin and doxorubicin. It is anticipated that compound **10** will be safer than both the standard drugs (Table 1).

3.2.2. Soft agar colony assay

The antiproliferative activity of carbamate derivative **10** was further substantiated by Soft agar colony formation assay in MDA-MB-231 cells. This assay is considered the most astringent assay for detecting the malignant transformation of cells. It is semi-quantitative and used to measure morphological transformation of cancer cell colonies induced by the test drug. In assay, compound **10** inhibited growth formation of colonies of breast cancer cells in a concentration dependent manner even after 16 days of incubation (Table 2). The breast cancer cell colony was reduced by 5.9–61.1% at 2–50 μg/mL concentrations. However, this effect was much less than doxorubicin.

3.2.3. Cell cycle analysis

The fundamental aim of cell cycle is to replicate DNA followed by cell division. It is an ordered process which is very much distressed in case of cancer cells. In cell cycle analysis in MDA-MB-231 cells, carbamate **10**, exerted G1 phase arrest and induces apotosis (Table 3). At its double IC_{50} and quadruple IC_{50} compound **10** significantly enhanced apoptosis by several folds as compared to control (Fig. S1, Supplementary information).

Table 3
MDA-MB-231 cells arrest by compound **10** in cell cycle analysis.

Compound	Concentration (μg/mL)	Average Percent Population of Cells			
		Apoptosis	G0/G1	S	G2/M
Control	—	2.60 ± 0.28	77.70 ± 0.28	11.35 ± 0.07	8.35 ± 0.07
10	3.95 (Half IC_{50})	1.25 ± 0.21	81.70 ± 0.71	7.70 ± 0.28	9.35 ± 0.21
	7.90 (IC_{50})	2.60 ± 0.28	81.05 ± 0.21	5.90 ± 0.14	10.50 ± 0.28
	15.80 (Double IC_{50})	49.45 ± 0.07	37.35 ± 0.07	6.85 ± 0.07	6.35 ± 0.21
	31.60 (Quadruple IC_{50})	88.20 ± 0.28	8.10 ± 0.14	2.20 ± 0.14	1.50 ± 0.28
Doxorubicin	1.0	3.15 ± 0.07	5.90 ± 0.14	1.70 ± 0.14	89.25 ± 0.07

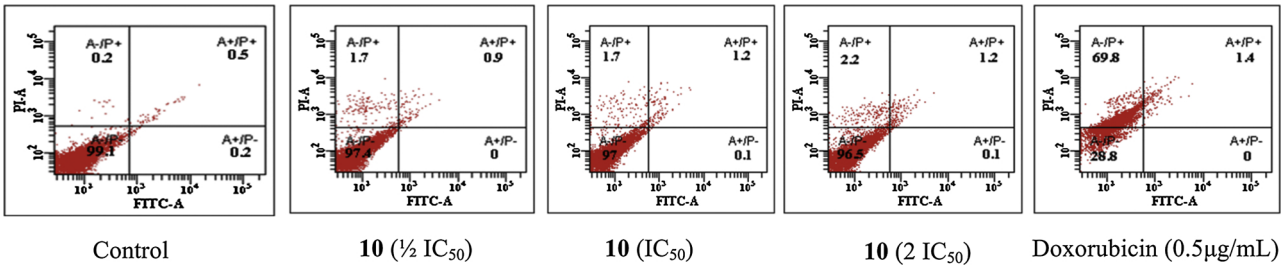

Fig. 3. Compound **10** induces late apoptosis in MDA-MB-231 cells.
MDA-MB-231 cells were incubated with compound **10** at the indicated concentrations for 24 h followed by staining with Annexin V-FITC/PI and analyzed for apoptotic and necrotic cell populations from flow cytometer within one hour.

*3.2.4. Apoptosis vs Necrosis induction by **10** by Annexin V-FITC assay*

The carbamate derivative of diosgenin **10** did not induce any early apoptosis in the MDA-MB-231 cells at its half IC_{50} (6.75 μM), IC_{50} (13.5 μM), double IC_{50} (27 μM). However, it induces late apoptosis by 0.9%, 1.2% and 1.2% respectively. It is worth to mention that necrosis level was reduced by compound **10** and late apoptosis was enhanced as compared to control experiment (without treatment) which clearly indicates apoptosis induction in MDA-MB-231 through a systematic pathway or a well defined mechanism (Fig. 3).

3.2.5. Molecular docking studies

The molecular docking studies shows that compounds **10** and doxorubicin actively bound within the active site of the caspase-3 and caspase-9 proteins 3D structures and showed the binding energy of -9, -8.5, and -8.1 kcal/mol with caspase-3 and binding energy of -8.4, -7.6, and -7.4 kcal/mol with caspase-9 as shown in Tables 4A and 4B . All the docked compounds also showed hydrogen bonding with their interacting amino acid residues and also shared common interacting residues (Fig. S2A and S2B, Supplementary information). It stipulates the induction of apoptosis in MDA-MB-231 cells through caspase signalling cascade.

The assessment for Lipinski's rule of five showed that compound **10** (two violations, higher molecular weight 584.83 and higher log P value) and doxorubicin (three violations, higher molecular weight, H-donors & H-acceptors) (Table 5).

*3.2.6. Apoptosis induction by carbamate **10** by caspase signalling cascade*

In caspase-3 activation assay, compound **10** exhibited activation of caspase-3 in MDA-MB-231 cells by 9.88% at its double IC_{50} (27 μM) concentration to induce apoptosis (Table 6). While the standard drug, doxorubicin had much higher induction to activate caspase-3 (36.7% at 1 μM and 51.4% at 2 μM). The activation of caspase-3 by compound **10** was relatively low as compared to doxorubicin. Caspase-3 is a critical promoter of apoptosis.

*3.2.7. Anti-inflammatory activity of furostene carbamates **6** and **10***

Deregulatory inflammation plays a pivotal role in the initiation, development and progression of tumour [34]. Diosgenin based carbamate derivatives **6** and **10** significantly inhibited LPS-stimulated productions of pro-inflammatory cytokines, thus exhibiting anti-inflammatory activity as well (Table 7) (Fig. S3, Supplementary information). Compound **10** exhibited IL-6 inhibition better than doxorubicin. But both the compounds had relatively lower activity than the standard anti-inflammatory drug dexamethasone.

3.2.8. In-vivo efficacy by Ehrlich ascites carcinoma

The Ehrlich Ascites Carcinoma is a well established model in tumour biology which is extensively used to study the tumour pathogenesis and development of anticancer agents [35,36]. The compound **10** was evaluated for its *in-vivo* efficacy by Ehrlich Ascites Carcinoma (EAC). There was no adverse effect on mice bodyweight (Table 8). It showed significant *in-vivo* efficacy in mice model by reducing 54.4% EAC tumour at 50 mg/kg *i.p.* dose. While, this effect was higher at 75 mg/kg dose where it reduced 65.4% EAC tumour by same route of administration (Table 9) (Fig. S4, Supplementary information). However, the control drug 5-fluorouracil exhibited potential activity at 20 mg/kg by reducing 96% tumour. There was no mortality of animals in any of the experimental group.

3.2.9. Safety studies

In acute oral toxicity experiment, compound **10** was found to be quite safe and well tolerated by mice. There were no observational changes, morbidity and mortality throughout the experimental period up to the dose level of 1000 mg/kg body weight. No morbidity or any other gross observational changes could be noticed in the group of animals treated with the test drug at 1000 mg/kg. The blood and serum samples upon analysis showed non-significant changes in all the parameters studied like total haemoglobin level, RBC count, WBC count, differential leucocytes count, ALP, SGPT, serum protein, albumin, creatinine, triglycerides, and cholesterol, (Table 10 and Fig. 4). On gross pathological study, animals did not show any changes in the organs studied including their absolute and relative organ weights (Fig. 5). However, there were some minor issues of slight enhancement in SGOT and triglyceride levels which is very much possible in case of a cytotoxic drug when orally ingested. Overall, the experiment showed that carbamate **10** is well tolerated by the Swiss albino mice up to the dose level of 1000 mg/kg body weight as a single acute oral dose. However, sub-acute and chronic experiments with the test drug need to

Table 4A
Compound **10** and doxorubicin both occupy similar binding pocket in Caspase-3 (PDB ID: 3KJF).

S. No	Compound	Docking Energy Kcal/Mol	Residues with in region of 4 Å radius	H-bond forming residues bond length in Å
1	**10**	−9	MET 61, HIS 121, GLY 122, CYS 163, TYR 204, **TRP 206**, **ARG 207**, **ASN 208**, TRP 214, **GLU 248**, SER 249, **PHE 250**, PHE 256	HIS 121 (3.05), TRP 214 (2.8), PHE 250 (3.2)
2	Doxorubicin	−8.1	THR 62, HIS 121, CYS 162, SER 205, **TRP 206**, **ARG 207**, **ASN 208**, TRP 214, **GLU 248**, **PHE 250**	ARG 207 (2.9)

Table 4B
Compound **10** and doxorubicin both occupy similar binding pocket in Caspase-9 (PDB ID: INW9).

S. No	Compound	Docking Energy (Kcal/Mol)	Residues with in region of 4 Å radius	H-bond forming residues bond length in Å
1	**10**	−8.4	**LEU 244**, **GLN 245**, VAL 264, ASN 265, PHE 267, ASN 268, GLY 269, LYS 280,**GLY 304**, GLY 305, **GLY 306**, **PHE 319**, **GLN 320**, **TYR 324**, THR 337, PRO 338, SER 339, ILE 341,	GLY 269 (3.1)
2	Doxorubicin	−7.4	SER 242, HIS 243, **LEU 244**, **GLN 245**, ARG 258, GLU 261, LYS 299, HIS 302, **GLY 304**, **GLY 306**, PRO 318, **PHE 319**, **GLN 320**, **TYR 324**	GLN 245 (3), ARG 258 (2.9), GLU 261 (3.1)

Table 5
Druggability of compound **10** (oral bioavailability) through Lipinski's rule of five. (It shows only two violations, better than doxorubicin).

Compound	Molecular weight (≤500)	Log P (≤5)	H-bond donors (≤5)	H-bond acceptors (≤10)	Rule of 5 violations allowed (≤1)
10	584.83	5.56	0	7	2
Doxorubicin	541.546	0.43	7	11	3

Table 6
Activation of Caspase-3 by compound **10** and doxorubicin.

S. No.	Compound	Concentration	Activation of Caspase-3 (%)
1.	**10**	13.52 μM (IC_{50})	—
2.	**10**	27.024 μM (Double IC_{50})	**9.88**
3.	Doxorubicin	1.0 μM	36.73
4.	Doxorubicin	2.0 μM	51.37

be carried out to look for any adverse effect on repeated exposure of the test drug **10** for its future development.

4. Discussion

Breast cancer is a heterogeneous disease. The clinical management of triple negative breast cancer (TNBC) is challenging due to relatively more aggressive biological behaviour and paucity of specific target. Nevertheless, the disease is tackled with a wide range of cytotoxic drugs by chemotherapy [5].

Diosgenin is a steroidal sapogenin possessing a spiroketal linkage. We synthesized several carbamates after opening spiroketal ring (F-ring) of diosgenin. In drug design, carbamates are important class of organic compounds possessing anticancer activity [37,38,39]. Chemically, it bears an amide-ester hybrid structure (R-*O*-CO-N-R') which functionally displays very good chemical and proteolytic stabilities. It has an ability to modulate inter- and intra- molecular interactions with target enzymes or receptors due to its surrogate peptidic bond [37]. Further, carbamate group also participates in hydrogen bonding through carbonyl group and two other heteroatoms. Thus, it has an ability to induce a biological response and favourable pharmacokinetic properties of the ligand. In the present series of compounds, only one compound exhibited significant anticancer activity with adequate safety margin.

Cell cycle is an important phenomenon for cell growth and proliferation in mammalian cells. It is regulated by some of the regulatory proteins and checkpoints to maintain genomic integrity. However, in cancerous cells the signalling system of cells is disrupted and cells keep on proliferating due to malfunctioning of cell cycle regulators. Carbamate **10** exhibited cell cycle arrest at G1 phase which ultimately inhibits DNA duplication in MDA-MB-231 cells. On treatment with carbamate **10**, cancer cells initiated apoptosis which was significantly high at double and quadruple IC_{50}. The induction of cell cycle arrest in breast cancer cells might be through various mechanisms. Induction of cell cycle arrest and reinstate apoptosis in cancer cells is one of the most widespread strategies to terminate cancer advancement [40].

In molecular docking studies, carbamate **10** showed good binding affinity with both the protease enzymes *i.e.* caspase-3 and caspase-9, comparable to standard drug doxorubicin. In the docked view with caspase-3, there were five residual amino acids common to both compound **10** and doxorubicin indicating the occupancy of same binding pocket. Similarly, there were seven amino acid residues common to compound **10** and doxorubicin in the docked view of caspase-9. Carbamate **10** activated caspase-3 to induce apoptosis in breast cancer cells. Evasion of apoptosis is considered to be one of the hallmarks of cancers [41]. Caspases are primary drivers of apoptotic cell death. Caspases are a family of cysteine dependent aspartate specific proteases that play crucial role in the maintenance of organism homeostasis throughout the life [42]. Caspases are key mediators of inflammatory response and apoptosis [42]. Functionally, there are two types of caspase, 'initiators' and 'effectors'. Initiator caspase are caspases-2, 8, 9 and 10 while, effector caspases are caspase-3, 6, and 7. Caspases induce apoptosis through cleavage of numerous proteins ultimately leading to the phagocytic recognition and engulfment of dying cells. Carbamate **10** activated caspase-3 in triple negative breast cancer cells. But, this effect was very weak. Down-regulation of caspase-3 has been a possible reason for drug resistance in breast cancer cases [43].

Tumour related macrophages are key regulators that link between cancer and inflammation. It is well established now that chronic inflammation leads to cancer progression [44]. In breast cancer patients high levels of TNF-α and IL-6 have been prognostic biomarkers linked with inflammation induced breast cancer [45]. Carbamate **10** inhibited over-expressions of TNF-α and IL-6, by 33.68% and 49.10% respectively at 10 μg/mL concentration. Thus, it exhibited moderate anti-inflammatory activity which is an advantageous property of carbamate **10**. Pro-inflammatory cytokines TNF-α and interleukins have been well demonstrated to contribute to inflammation associated carcinogenesis [34,46,47]. TNF-α and IL-6 have been over-expressed in a variety of tumour cells including breast cancer [47,48]. Tumour microenvironment plays an important role in cancer chemotherapy [49]. Hence, down-regulation of these cytokines by carbamate **10** may reduce the aggressiveness of the disease and will be useful in cancer therapy. Overall, the induction of apoptosis by compound **10** in MDA-MB-231 cells might be due to activation of caspase-3 and also by inhibiting inflammatory cytokines. However, both the effects were moderate to weak.

'*Lipinski rule of* 5' is a thumb rule to assess druggability of a lead compound to reduce attrition in drug discovery and development [50a,50b]. These are four physical properties; molecular weight, log P,

Table 7
Moderate antiinflammatory activities of compounds **6** and **10** on production of LPS-induced pro-inflammatory cytokines in primary macrophage cells.

Compound	LPS (0.5 μg/mL)	Dose (μg/mL)	TNF-α (pg/mL) Mean ± SE	% Inhibition of TNF-α	IL-6(pg/mL) Mean ± SE	% Inhibition of IL-6
Normal	–	—	126.38 ± 29.36	NA	173.88 ± 23.73	NA
Vehicle	√	—	975.08 ± 16.34$^{\#}$	00	843.31 ± 43.88$^{\#}$	00
6	√	1μg	818.36 ± 31.95*	16.07 ± 3.27	727.28 ± 37.86*	13.75 ± 4.48
	√	10μg	700.90 ± 24.65*	**28.11 ± 2.52**	658.83 ± 41.22*	21.87 ± 4.88
10	√	1μg	758.80 ± 60.59*	22.18 ± 6.21	561.91 ± 35.96*	33.36 ± 4.26
	√	10μg	646.86 ± 16.89*	**33.66 ± 1.73**	429.21 ± 26.14*	**49.10 ± 3.09**
Doxorubicin	√	1μg	661.88 ± 31.13*	32.12 ± 3.19	548.75 ± 22.01*	34.92 ± 2.60
	√	10μg	516.80 ± 23.71*	**46.99 ± 2.43**	502.76 ± 24.08*	**40.38 ± 2.85**
Dexamethasone	√	1μg	377.03 ± 25.85*	61.33 ± 2.65	318.86 ± 15.98*	**62.18 ± 1.85**
	√	10μg	267.38 ± 32.20*	**72.57 ± 3.30**	214.50 ± 21.22*	**74.56 ± 2.51**

Normal *vs* Vehicle; $^{\#}$ $P < 0.05$; Vehicle *vs* Treatment; ^{ns}not significant *$P < 0.05$, n = 3.

Table 8
Body-weight of Swiss albino mice during *in-vivo* anticancer activity (EAC) of compound **10.**

Body weight (g)					
Sample	Dose	Day 1	Day 5	Day 9	Day 12
Control	NS (0.2 mL), i.p.	24.00 ± 0.45	25.20 ± 0.66	26.80 ± 0.66	27.40 ± 0.60
Compound **10**	50 mg/kg, i.p.	24.00 ± 0.51	25.75 ± 0.97	28.75 ± 1.14	29.93 ± 0.84
	75 mg/kg, i.p.	23.80 ± 0.86	26.00 ± 1.22	28.40 ± 1.78	25.33 ± 2.17
5-Fluorouracil	20 mg/kg, i.p.	20.20 ± 0.37	25.20 ± 0.66	26.80 ± 0.66	27.40 ± 0.60

Table 9
Compound **10** exhibits significant reduction of tumour in *in-vivo* anticancer activity of against Ehrlich Ascites Carcinoma.

Compound	Dose (mg/kg, i.p.)	Tumour Volume (mL) Mean ± S.E.	Tumour weight (g) Mean ± S.E.	Tumour cell count (1×10^7) Mean ± S.E.	Tumour growth Inhibition (%)
Control	NS (0.2 ml)	6.4 ± 0.74	6.47 ± 0.77	71.8 ± 7.72	—
Compound **10**	50 mg/kg	4.6 ± 1.17	4.81 ± 1.25	32.75** ± 4.02	54.38
Compound **10**	75 mg/kg	2.26* ± 0.48	2.10* ± 0.49	24.85** ± 2.74	**65.39**
5-Fluorouracil	20 mg/kg	0.21** ± 0.09	0.22** ± 0.09	2.35** ± 0.99	**96.72**

*Significant (p = < 0.05), **Highly significant (p = < 0.01) by Dunnett's test, data are mean ± S.E. (n = 5).

Table 10
Non-toxic effects on haematological and serum biochemical parameters by compound **10** in Swiss-albino mice.

Parameters		Dose of 10 at mg/kg body weight as a single oral dose				
		Control	5 mg/kg	50 mg/kg	300 mg/kg	1000 mg/kg
Body weight (g)		29.80 ± 2.22	29.11 ± 1.35	28.26 ± 0.71	27.68 ± 1.33	32.62 ± 0.30
Haematological Parameters	**Haemoglobin (g/dL)**	14.19 ± 2.41	12.56 ± 1.28	12.48 ± .52	12.86 ± 0.32	12.90 ± 0.76
	RBC (million/mm^3)	6.64 ± 0.32	6.49 ± 0.46	7.14 ± 0.44	6.49 ± 0.26	5.69 ± 0.49
	WBC (1000*/mm^3)	3.44 ± 0.32	4.39 ± 0.28	4.56 ± 0.55	4.43 ± 0.50	4.77 ± 0.33
Liver Function Test	**ALP (U/L)**	68.28 ± 9.12	53.72 ± 4.38	89.38 ± 17.07	75.96 ± 9.35	60.59 ± 11.24
	SGOT (U/L)	34.61 ± 3.05	46.98 ± 4.38	39.82 ± 3.88	44.00 ± 3.93	**52.37 ± 9.11**
	SGPT (U/L)	16.63 ± 1.85	15.44 ± 3.16	13.19 ± 7.95	16.05 ± 5.78	15.72 ± 1.88
	Albumin (g/dL)	3.17 ± 0.20	2.64 ± 0.29	2.95 ± 0.14	3.21 ± 0.11	3.18 ± 0.11
	Bilirubin (mg/dL)	0.63 ± 0.06	0.48 ± 0.08	0.52 ± 0.03	0.46 ± 0.02	0.68 ± 0.06
	Serum Protein (mg/mL)	6.07 ± 0.40	5.54 ± 0.38	6.14 ± 0.33	6.10 ± 0.13	6.57 ± 0.30
Kidney Function Test	**Creatinine (mg/dL)**	1.21 ± 0.26	1.20 ± 0.25	1.47 ± 0.34	1.62 ± 0.41	1.27 ± 0.27
Lipid Profile	**Triglycerides (mg/dL)**	98.36 ± 6.66	95.46 ± 5.96	94.88 ± 6.31	99.63 ± 5.14	**123.07 ± 9.84**
	Total Cholesterol (mg/dL)	218.94 ± 19.46	171.97 ± 11.87	179.55 ± 13.44	173.23 ± 8.79	169.44 ± 15.17

Data are expressed as Mean ± SE (n = 6). SGOT: serum glutamic-oxaloacetic transaminase, SGPT: Serum glutamic pyruvic transaminase ALP: Alkaline phosphatase.Tukey's multiple comparison test was used to determine the significance between compound **10** and control, P < 0.001.

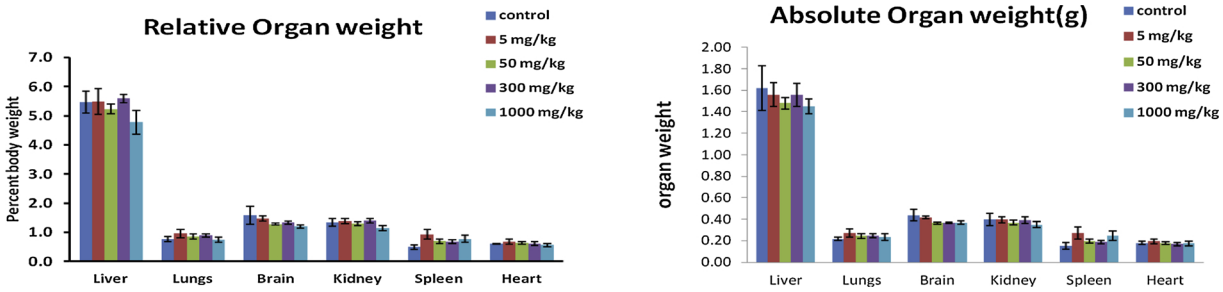

Fig. 4. Compound **10** does no affect on absolute and relative organ weights in Swiss albino mice.
Acute oral dose of compound **10** at 5, 50, 300 and 1000 mg/kg body weight, followed protocol as described in materials and methods section (n = 6, Non significant changes were found compared to control by Tukey's test; compound **10** is well tolerable and safe in Swiss-albino mice up to 1000 mg/kg dose**).**

hydrogen bond donors and acceptors. Generally one deviation is acceptable, but compound **10** showed two deviations. Nowadays, there is an approach *i.e.* '*beyond rule of five*' as Lipinski rule provides very narrow chemical space to fulfil the rule. In the recent years an increasing number of successful new drugs have been launched that significantly violate these empirical rules, and it is apparent the principles for the successful design of '*beyond rule of five*' drugs are poorly understood [51]. There are many successful drugs larger in size, highly hydrophobic through a fundamentally different route. Certainly, small molecules have high chances of aqueous solubility and also be absorbed through the gut and penetrate cells, while, larger molecules cannot. The low solubility of larger molecules, combines with high protein binding, means that these molecules inevitably will have low unbound free fractions and circulated through the target organ by serum proteins [51]. Sometimes, lymphatic transport plays a significant role in the transportation of lipid soluble drugs [52].

Compound **10** exhibited potent *in-vivo* efficacy in Ehrlich ascites carcinoma studies. EAC is an undifferentiated carcinoma with 100%

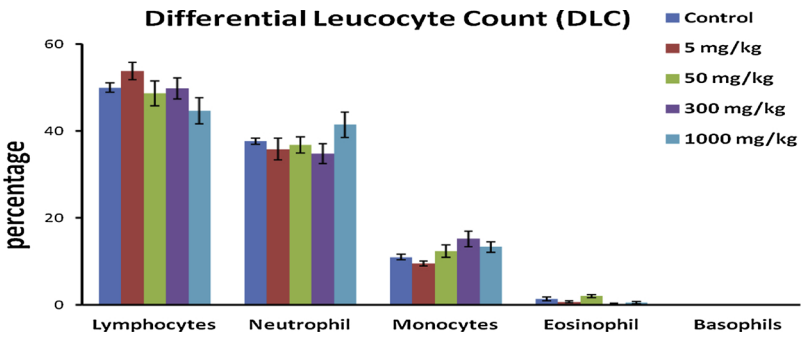

Fig. 5. No changes on differential leucocyte counts by compound **10.** Acute oral dose of compound **10** at 5, 50, 300 and 1000 mg/kg body weight in Swiss albino mice, followed protocol as described in materials and methods section (n = 6, Non significant changes were found compared to control by Tukey's test; compound **10** is well tolerable and safe up to 1000 mg/kg dose**).**

tumourigenicity which is difficult to treat [53]. The efficacy of carbamate **10** in EAC model was less than the standard drug 5-fluorouracil. However, the toxicity of compound **6a** was relatively much less than 5-fluorouracil.

Pharmacovigilance or drug safety is an important aspect in drug development, mainly focusing on adverse drug reactions. The safety-efficacy ratio of an investigational drug is crucial in assessing risk-benefit for decision making during clinical use [54]. In acute oral toxicity, the test compound is given to experimental animals for a short period of time. The estimation of rodent acute toxicity is a crucial task in safety assessment of the drug candidate. Carbamate **10** was well tolerated and found safe up to 300 mg/kg dose. However, there were some minor issues of enhanced SGOT and triglyceride levels at 1000 mg/kg dose. In view of minor issues at higher dose of compound **10**, it should be evaluated for sub-acute, chronic or sub-chronic experiments for any adverse effect on prolonged exposure. The safety evaluation is increasingly being recognised as a key dimension for successful drug development due to changing societal, legal and regulatory expectations [55].

5. Conclusion

TNBC is currently a subset of breast cancer with limited therapeutic options and hence adverse clinical outcome. In the present study, diosgenin has been modified to obtain several new carbamate derivatives. Furostene carbamate derivative **10** inhibited triple negative breast cancer cells significantly by arresting cell cycle at G1 phase and induced apoptosis by activating caspase-3. Thus, carbamate **10** exhibits antiproliferative activity by inducting apoptosis through caspase pathway. It reduces LPS induced inflammation by lowering the expression of cytokines, TNF-α and IL-6 significantly. *In-vivo* efficacy of carbamate **10** was moderate and safe up to 300 mg/kg oral dose in rodents. Overall, the study provides a dual action diosgenin based furostene carbamate derivative against inflammatory cancers and/or inflammation induced carcinogenesis with sufficient therapeutic window. Presently, optimization studies are underway to get better carbamate derivative.

Declaration of Competing Interest

The authors declare no conflict of interest.

Acknowledgement

The study is financially supported from National Medicinal Plant Board (NMPB), Ministry of AYUSH, Government of India through GAP-333. Ms. Kaneez Fatima acknowledges CSIR for her Senior Research Fellowship. Biological Central Facility and Chemical Central Facility of CSIR-CIMAP are duly acknowledged for Sophisticated Instrument support. SAIF CSIR-CDRI is also acknowledged for high resolution mass analysis (APCI-TOF).

Appendix A. Supplementary data

Supplementary material related to this article can be found, in the online version, at doi:https://doi.org/10.1016/j.jsbmb.2019.105457.

References

[1] WHO Cancer Factsheet, (2018) 12 September.
[2] D.L. Holliday, V. Speirs, Choosing the right cell line Fig. 4for breast cancer research, Breast Cancer Res. 13 (2011) 215.
[3] M. Al-Hajj, M.S. Wicha, A. Benito-Hernandez, S.J. Morrison, M.F. Clarke, Prospective identification of tumourigenic breast cancer cells, Proc. Natl. Acad. Sci. U. S. A. 100 (2003) 3983–3988.
[4] G. Bianchini, J.M. Balko, I.A. Mayer, M.E. Sanders, L. Gianni, Triple negative breast cancer: challenges and opportunities of a heterogeneous disease, Nat. Rev. Clin. Oncol. 13 (2016) 674–690.
[5] F. Pado, L.M.C. Buydens, H. Degani, R. Hilhorst, E. Klipp, I.S. Gribbestad, S.V. Huffel, H.W.M. van Laarhoven, J. Luts, D. Monleon, G.J. Postma, N. Schneiderhan-Narra, F. Santoro, H. Wouters, H.G. Russnes, T. Sorlie, E. Tagliabue, A.L. Borresen-Dale, Triple negative breast cancer: present challenges and new perspectives, Mol. Oncol. 4 (2010) 209–229.
[6] N. Berrada, S. Delaloge, F. André, Treatment of triple-negative metastatic breast cancer: toward individualized targeted treatments or chemosensitization? Ann. Oncol. 21 (2010) vii30–vii35.
[7] US-FDA: https://www.fda.gov/Drugs/InformationOnDrugs/ApprovedDrugs/ucm592357.htm.
[8] Chinese patent, CN105440094A, Preparation method of dexamethasone intermediate.
[9] C. Djerassi, Steroid research at Syntex: "the pill" and cortisone, Steroids 57 (1992) 631–641.
[10] P. Aumsuwan, S.I. Khan, I.A. Khan, Z. Ali, B. Avula, L.A. Walker, Z. Shariat-Madar, W.G. Helferich, B.S. Katzenellenbogen, A.K. Dasmahapatra, The anticancer potential of steroidal saponin, dioscin, isolated from wild yam (*Dioscorea villosa*) root extract in invasive human breast cancer cell line MDA-MB-231 *in vitro*, Archiv. Biochem. Biophys. 591 (2015) 98–110.
[11] W.C. Lim, H. Kim, Y.J. Kim, K.C. Choi, I.H. Lee, K.H. Lee, M.K. Kim, H. Ko, Dioscin suppresses TGF-b1-induced epithelial-mesenchymal transition and suppresses A549 lung cancer migration and invasion, Bioorg. Med. Chem. Lett. 27 (2017) 3342–3348.
[12] G. Zhang, X. Zeng, R. Zhang, J. Liu, W. Zhang, Y. Zhao, X. Zhang, Z. Wu, Y. Tan, Y. Wu, B. Du, Dioscin suppresses hepatocellular carcinoma tumour growth by inducing apoptosis and regulation of TP53, BAX, BCL2 and cleaved CASP3, Phytomed. 23 (2016) 1329–1336.
[13] X. Zhao, L. Xu, L. Zheng, L. Yin, Y. Qi, X. Han, Y. Xu, J. Peng, Potent effects of dioscin against gastric cancer *in vitro* and in vivo, Phytomed. 23 (2016) 274–282.
[14] Y. Wang, Q.Y. He, J.F. Chiu, Dioscin induced activation of p38 MAPK and JNK via mitochondrial pathway in HL-60 cell line, Eur. J. Pharmacol. 735 (2014) 52–58.
[15] L. Si, L. Zheng, L. Xu, L. Yin, X. Han, Y. Qi, C. Wang, J. Peng, Dioscin suppresses human laryngeal cancer cells growth *via* induction of cell-cycle arrest and MAPK-mediated mitochondrial-derived apoptosis and inhibition of tumour invasion, Eur. J. Pharmacol. 774 (2016) 105–117.
[16] S. Mu, X. Tian, Y. Ruan, Y. Liu, D. Bian, C. Ma, C. Yu, M. Feng, F. Wang, L. Gao, J.J. Zhao, Diosgenin induces apoptosis in IGF-1-stimulated human thyrocytes through two caspase-dependent pathways, Biochem. Biophys. Res. Commun. 418 (2012) 347–352.
[17] B. Cai, K.J. Seong, S.W. Bae, C. Chun, W.J. Kim, A synthetic diosgenin primary amine derivative attenuates LPS-stimulated inflammation *via* inhibition of NF-κB and JNK MAPK signaling in microglial BV2 cells, Int. Immunopharmacol. 61 (2018) 204–214.
[18] A. Binesh, S.N. Devaraj, D. Halagowder, Atherogenic diet induced lipid accumulation induced NFκB level in heart, liver and brain of Wistar rat and diosgenin as an anti-inflammatory agent, Life Sci. 196 (2018) 28–37.
[19] Z. He, H. Chen, G. Li, H. Zhu, Y. Gao, L. Zhang, J. Sun, Diosgenin inhibits the migration of human breast cancer MDA-MB-231 cells by suppressing Vav2 activity, Phytomed. 21 (2014) 871–876.
[20] S. Jiang, J. Fan, Q. Wang, D. Ju, M. Feng, J. Li, Z. bin Guan, D. An, X. Wang,

Diosgenin induces ROS-dependent autophagy and cytotoxicity via mTOR signalling pathway in chronic myeloid leukaemia cells, Phytomed. 15 (2016) 243–252.
[21] F. Li, P.P. Fernandez, P. Rajendran, K.M. Hui, G. Sethi, Diosgenin, a steroidal saponin, inhibits STAT3 signaling pathway leading to suppression of proliferation and chemosensitization of human hepatocellular carcinoma cells, Cancer Lett. 292 (2010) 197–207.
[22] C. Lepage, D.Y. Leger, J. Bertrand, F. Martin, J.L. Beneytout, B. Liagre, Diosgenin induces death receptor-5 through activation of p38 pathway and promotes TRAIL-induced apoptosis in colon cancer cells, Cancer Lett. 301 (2011) 193–202.
[23] M.A. Fernandez-Herrera, H. Lopez-Munoz, J.M.V. Hernandez-Vazquez, M. Lopez-Davila, M.L. Escobar-Sanchez, L. Sanchez-Sanchez, B.M. Pint, J. Sandoval-Ramirez, Synthesis of 26-hydroxy-22-oxocholestanic frameworks from diosgenin and hecogenin and their in vitro antiproliferative and apoptotic activity on human cervical cancer CaSki cells, Bioorg. Med. Chem. 18 (2010) 2474–2484.
[24] a) A.A. Hamid, Mohammad Hasnain, Arjun Singh, Omprakash, Prema G. Vasudev, Jayanta Sarkar, Debabrata Chanda, Feroz Khan, O.O. Aiyelaagbe, Arvind S. Negi, Synthesis of novel anticancer agents through opening of spiroketal ring of diosgenin, Steroids 87 (2014) 108–118;
b) M. Singh, A.A. Hamid, A.K. Maurya, O. Prakash, F. Khan, A. Kumar, O.O. Aiyelaagbe, A.S. Negi, D.U. Bawankule, Synthesis of diosgenin analogues as potential anti-inflammatory agents, J. Steroid Biochem. Mol. Biol. 143 (2014) 323–333;
c) A.A. Hamid, Tanu Kaushal, Raghib Ashraf, Arjun Singh, Amit Chand Gupta, Prakash Om, Jayanta Sarkar, Debabrata Chanda, D.U. Bawankule, Feroz Khan, Karuna Shanker, O.O. Aiyelaagbe, Arvind S. Negi, (22β,25R)-3β-Hydroxy-spirost-5-en-7-iminoxy-heptanoic acid exhibits anti-prostate cancer activity through caspase pathway, Steroids 119 (2017) 43–52.
[25] G.P. Moss, “The nomenclature of steroids”. IUPAC and international union of biochemistry and molecular biology-joint commission on biochemical nomenclature, Pure Appl. Chem. 61 (1989) 1783–1822.
[26] S. Khwaja, K. Fatima, M. Hassanain, C. Behera, A. Kour, A. Singh, S. Luqman, J. Sarkar, D. Chanda, K. Shanker, A.K. Gupta, D.M. Mondhe, A.S. Negi, Antiproliferative efficacy of curcumin mimics through microtubule destabilization, Eur. J. Med. Chem. 151 (2018) 51–61.
[27] W. Kakuguchi, T. Kitamura, T. Kuroshima, M. Ishikawa, Y. Kitagawa, Y. Totsuka, M. Shindoh, F. Higashino, HuR knockdown changes the oncogenic potential of oral cancer cells, Mol. Cancer Res. 8 (2010) 520–528.
[28] C. Riccardi, I. Nicoletti, Nat. Protoc. 1 (2006) 1458–1461.
[29] C.Y. Looi, A. Arya, F.K. Cheah, B. Muharram, K.H. Leong, et al., Induction of apoptosis in human breast cancer cells via caspase pathway by vernodalin isolated from *Centratherum anthelminticum* (L.) seeds, PLoS One 8 (2013) e56643.
[30] a) O. Trott, A.J. Olson, AutoDock Vina: improving the speed and accuracy of docking with a new scoring function, efficient optimization, and multithreading, Sdrp J. Comput. Chem. Mol. Model. 31 (2010) 455–461;
b) Z. Wang, W. Watt, N.A. Brooks, M.S. Harris, J. Urban, D. Boatman, M. McMillan, M. Kahn, R.L. Heinrikson, B.C. Finzel, A.J. Wittwer, Kinetic and structural characterization of caspase 3 and caspase 8 inhibition by a novel class of irreversible inhibitors, Biochim. Biophys. Acta (BBA)-Proteins Proteomics 1804 (2010) 1817–1831;
c) E.N. Shiozaki, J. Chai, D.J. Rigotti, S.J. Riedl, S.M. Srinivasula, E.S. Alnemri, R. Fairman, Y. Shi, Mechanism of XIAP-mediated inhibition of caspase-9, Mol. Cell 11 (2003) 519–527;
d) R.A. Laskowski, M.B. Swindells, LigPlot+: multiple ligand–protein interaction diagrams for drug discovery, J. Chem. Inf. Model. 51 (2011) 2778–2786.
[31] H.R. Stennicke, C.A. Ryan, G.S. Salvesen, Reprieval from execution: the molecular basis of caspase inhibition, Trends Biochem. Sci. 27 (2002) 94–101.
[32] J.J. Allan, A. Damodaran, N.S. Deshmukh, K.S. Goudar, A. Amit, Safety evaluation of a standardised phytochemical composition extracted from *Bacopa monnieri* in Sprague-Dawley rats, Food Chem. Toxicol. 45 (2007) 1928–1937.
[33] D. Chanda, K. Shanker, A. Pal, S. Luqman, D.U. Bawankule, D. Mani, M.P. Darokar, Safety evaluation of Trikatu, a generic Ayurvedic medicine in Charles Foster rats, J. Toxicol. Sci. 34 (2009) 99–108.
[34] E.Z.P. Chai, K.S. Siveen, M.K. Shanmugam, F. Arfuso, G. Sethi, Analysis of the intricate relationship between chronic inflammation and cancer, Biochem. J. 468 (2015) 1–15.
[35] M.F. Mota, P.L. Benfica, A.C. Batista, F.S. Martins, J.R. Paula, Investigation of Ehrlich ascites tumour cell death mechanisms induced by *Synadenium umbellatum* Pax, J. Ethnopharmacol. 139 (2012) 319–329.
[36] E.A. Saad, M.M. Hassanien, H.A. El-mezayen, N.M. ELmenawy, Regression of murine Ehrlich ascites carcinoma using synthesized cobalt complex, Med. Chem. Commun. 8 (2017) 1103–1111.
[37] A.K. Ghosh, M. Brindisi, Organic carbamates in drug design and medicinal chemistry, J. Med. Chem. 58 (2015) 2895–2940.
[38] S. Ray, D.D. Chaturvedi, Application of organic carbamates in drug design. Part 1: anticancer agents- recent reports, Drugs Fut. 29 (2004) 343–357.
[39] J.E. Cheong, M. Zaffagni, I. Chung, Y. Xu, Y. Wang, F.E. Jernigan, B.R. Zetter, L. Sun, Synthesis and anticancer activity of novel water soluble benzimidazole carbamates, Eur. J. Med. Chem. 144 (2018) 372–385.
[40] L.H. Hartwell, T.A. Weinert, Checkpoints: controls that ensure the order of cell cycle events, Science 246 (1989) 629–634.
[41] M. Olsson, B. Zhivotovsky, Caspases and cancer, Cell Death Differ. 18 (2011) 1441–1449.
[42] C.H. Wilson, S. Kumar, Caspase in metabolic disease and their therapeutic potential, Cell Death Differ. 25 (2018) 1010–1024.
[43] E. Devarajan, A.A. Sahin, J.S. Chen, R.R. Krishnamurthy, N. Aggarwal, A.M. Brun, et al., Down-regulation of caspase 3 in breast cancer: a possible mechanism for chemoresistance, Oncogene 21 (2002) 8843–8851.
[44] B.B. Aggarwal, S. Shishodia, S.K. Sandur, M.K. Pandey, G. Sethi, Inflammation and cancer: how hot is the link? Biochem. Pharmacol. 72 (2006) 1605–1621.
[45] C. Angoli, S. Grioni, V. Pala, A. Allione, G. Matullo, C.D. Gaetano, G. Tagliabue, S. Sieri, V. Krogh, Biomarkers of inflammation and breast cancer risk: a case control study nested in the EPIC-Varese cohort, Sci. Rep. 7 (2017) 12708.
[46] G. Sethi, B. Sung, A.B. Kunnumakkara, B.B. Aggarwal, Targeting TNF-α for treatment of cancer and autoimmunity, Adv. Exp. Med. Biol. 647 (2009) 37–51.
[47] K. Taniguchi, M. Karin, IL-6 and related cytokines as the critical lynchpins between inflammation and cancer, Semin. Immunol. 26 (2014) 54–74.
[48] S. Dalaklioglu, A. Tasatargil, S. Kale, G. Tanriover, S. Dilmac, N. Erin, Metastatic breast carcinoma induces vascular endothelial dysfunction in Balb-c mice: role of the tumour necrosis factor-α and NADPH oxidase, Vasc. Pharmacol. 59 (2013) 103–111.
[49] B. Lim, W.A. Woodward, X. Wang, J.M. Reuben, N.T. Ueno, Inflammatory breast cancer biology: the tumour microenvironment is key, Nature Rev. Cancer 18 (2018) 485–499.
[50] a) C.A. Lipinski, Lead- and drug-like compounds: the rule-of-five revolution, Drug Discov. Today Technol. 1 (2004) 337–341;
b) P.D. Leeson, B. Springthrope, The influence of drug like concepts on decision making in medicinal chemistry, Nat. Rev. Drug Discov. 6 (2007) 881–890.
[51] D.A. DeGoey, H.J. Chen, P.B. Cox, M.D. Wendt, Beyond the rule of 5: lessons learned from AbbVie’s drugs and compound collection, J. Med. Chem. 61 (2018) 2636–2651.
[52] E.F. Choo, J. Boggs, C. Zhu, J.W. Lubach, N.D. Catron, G. Jenkins, A.J. Souers, R. Voorman, The role of lymphatic transport on the systemic bioavailability of the Bcl-2 protein family inhibitors navitoclax (ABT-263) and ABT-199, Drug Metab. Dispos. 42 (2014) 207–212.
[53] H.W. Bearns, R.G. Kessel, Cancer Res. 28 (1968) 1944–1951.
[54] P.Y. Muller, M.N. Milton, The determination and interpretation of the therapeutic index in drug development, Nat. Rev. Drug Discov. 11 (2012) 751–761.
[55] A. Ray, Beyond debacle and debate: developing solutions in drug safety, Nat. Rev. Drug Discov. 8 (2009) 775–779.